Composite Materials and Engineering, *Vol. 4, No. 1 (2022) 101-115*
https://doi.org/10.12989/cme.2022.4.1.101

Numerical study on viscoelastic behavior of particulate composites based on the mean-field based micromechanics model

Hangil You[1] and Gun Jin Yun*[1,2]

[1]*Department of Aerospace Engineering, Seoul National University, Gwanak-gu, Seoul, 08826, Korea*
[2]*Institute of Advanced Aerospace Technology, Seoul National University, 08826, Seoul, Korea*

(Received August 6, 2021, Revised Fubruary 4, 2021, Accepted February 11, 2021)

Abstract. This paper investigates the effects of constituents' properties (i.e., stiffness ratio, volume fraction, and interfacial stiffness) on the viscoelastic behavior through the mean-field-based micromechanics model. The stress prediction of the proposed micromechanics model for the viscoelastic composites is verified through the direct numerical simulation (DNS) using a finite element model with different volume fractions, materials properties, and interphase layers. The stress prediction accuracy is studied under cyclic loading conditions. The stress prediction accuracy is better when the volume fraction is lower and the interphase layer is modeled. Finally, the effects of the constituent's properties, volume fraction, and interfacial imperfection on the tangent delta and relaxation behavior of the composites are examined.

Keywords: homogenization; Mori-Tanaka method; micromechanics; particulate composites; viscoelastic behavior

1. Introduction

Polymers with rubber-like mechanical behavior have a wide range of engineering applications, including tires, structural bearing, and medical devices thanks to their viscoelastic characteristics (Khajehsaeid *et al.* 2014). The rubber compound for tires is a composite material of the reinforced elastomer. Adding fillers such as carbon black (CB) to rubber compounds can strengthen the mechanical property, increase the volume, improve tire stiffness, and adjust dynamic mechanical properties (Oleiwi *et al.* 2011, Li *et al.* 2015, Khadimallah *et al.* 2020, Patnaik *et al.* 2020). Moreover, tires are manufactured through complex procedures such as mixing, extrusion, calendaring, beading, building, and vulcanization. Also, various chemical fillers with strengthening effects are added with varying volume fractions and interfacial integrity during the manufacturing processes (Park *et al.* 2020).

Consequently, it is necessary to reliably predict the rubber compound's viscoelastic stiffness and dynamic mechanical properties under various possible conditions (Shao *et al.* 2018). However, the experimental evaluation of the tire composites' dynamic mechanical properties and effective

*Corresponding author, Professor, E-mail: gunjin.yun@snu.ac.kr

http://www.techno-press.org/?journal=cme&subpage=7 ISSN: 2671-4930 (Print), 2671-5120 (Online)

materials properties is costly and time-consuming. Therefore, the computational approach is desirable to evaluate the tire composites' viscoelastic mechanical behavior under various conditions (Zhao *et al.* 2019).

Studies on the homogenization of composites using viscoelastic matrices have been conducted since 1960 for applications such as predicting the damping properties of rubber compounds. Previous studies in the literature are primarily divided into two methodologies: homogenizations in the Laplace domain and the time domain. Hashin first proposed homogenization of composites with viscoelastic matrix in the Laplace domain (Hashin 1965). The homogenization approach in the Laplace domain is beneficial in that the nonlinear characteristics of a viscoelastic material can be linearized in the Laplace domain according to the correspondence principle. Several homogenization methodologies in the Laplace domain are proposed with the convenience of calculating and estimating the effective properties of composites (Christensen 1969, Hashin 1970, Laws and McLaughlin 1978, Brinson and Lin 1998). However, the homogenization approach in the Laplace domain has some limitations. For example, effective mechanical properties are not always in a closed-form for the back transformation, and it is usually challenging to estimate the time domain response of viscoelastic composites. To overcome the above limitations, a methodology that conducts homogenization in the time domain is recently proposed. An approximate estimation method that uses the internal variable for homogenization in the time domain was first proposed by Lahellec *et al.* (Lahellec and Suquet 2007). Recently, Chen *et al.* proposed a micromechanics-based constitutive model that conducts homogenization in the time domain. (Chen *et al.* 2020). This approach decomposes the deformation, and the viscoelastic compound's long-term responses are utilized to formulate the constitutive model. The homogenization model based on the Laplace transformation provided convenience in estimating the effective material properties of composites. However, the time domain homogenization can obtain straightforward mechanical responses of the viscoelastic composite.

The objectives of the present study are as follows: 1) to numerically verify the three-dimensional viscoelastic micromechanics model with direct numerical simulation (DNS) FE models and 2) to investigate the effects of the compound's stiffness contrast, volume fraction, and interphase layer stiffness on the viscoelastic behavior of composites through the viscoelastic micromechanics model predicts. The micromechanics model for the time-domain Mori-Tanaka homogenization is formulated and described in Section 2. The finite element model and the DNS results are compared with the micromechanics model's results in Section 3. Through the verified micromechanics model, the effects of the stiffness ratio between the constituents, interfacial stiffness, and volume fractions on the dynamic mechanical property and relaxation behavior are investigated and discussed in Section 4. Finally, the results and findings of the research are summarized in the conclusion.

2. Micromechanics model for particulate composites

This section presents the micromechanics model of the viscoelastic composites. The Mori-Tanaka homogenization method based on Eshelby's inclusion theory is introduced.

2.1 Fundamentals of a micromechanical model

Fig. 1 shows the schematics of the particulate composites' representative volume element (RVE) with two kinds of elastic inclusion phases and a viscoelastic matrix. Fig. 1 is presented to show the

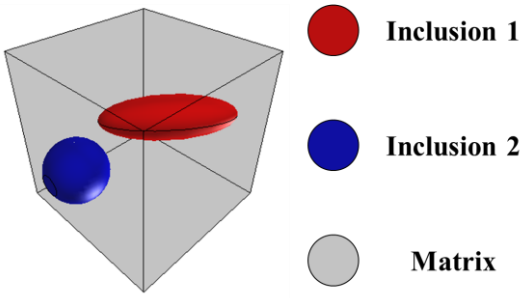

Fig. 1 Schematics of composite microstructure RVE with two kinds of inclusions

formulation of the Mori-Tanaka homogenization for general cases where there is more than one inclusion with various shapes. However, the particulate composite with only one spherical inclusion is examined in this research.

Consider the particulate composites with the N number of inclusions. Assuming that the macroscopic strain loads $\boldsymbol{\varepsilon}^{r}_{macro}$ is applied on the RVE, the effective stiffness of the micromechanical model $\boldsymbol{C}^{eff}_{macro}$ is obtained as

$$\mathbf{C}^{\text{eff}}_{\text{macro}} = \frac{1}{\Omega}\int_{\Omega} \mathbf{c}\,(\vec{\mathbf{r}}) : \mathbf{B}\,(\vec{\mathbf{r}})\mathrm{d}\Omega \tag{1}$$

where $\boldsymbol{c}\,(\vec{\boldsymbol{r}})$ and $\boldsymbol{B}\,(\vec{\boldsymbol{r}})$ are the local stiffness tensor and the global strain concentration tensor at an arbitrary position vector $\vec{\boldsymbol{r}}$ in a three-dimensional domain Ω. The effective stiffness $\boldsymbol{C}^{eff}_{macro}$ can be determined if the global strain concentration tensor $\boldsymbol{B}\,(\vec{\boldsymbol{r}})$ is obtained. A kinematic integral equation and modified Green tensor $\boldsymbol{\xi}$ can be utilized to obtain the global strain concentration tensor as follows (Dederichs and Zeller 1973)

$$\boldsymbol{\varepsilon}_{micro}(\vec{\boldsymbol{r}}) = \boldsymbol{\varepsilon}^{r}_{macro} - \int_{\Omega'} \boldsymbol{\xi}(\vec{\boldsymbol{r}} - \vec{\boldsymbol{r}}'): \delta\boldsymbol{C}_{fluc}\,(\vec{\boldsymbol{r}'})\boldsymbol{\varepsilon}_{micro}(\vec{\boldsymbol{r}}\,')d\Omega' \tag{2}$$

Herein, $\boldsymbol{C}_{fluc}$ is the fluctuation part of the stiffness that varies according to the arbitrary position vector $\vec{\boldsymbol{r}}$, and the notation: indicates the tensor contraction. The Ω' is a three-dimensional domain of the composite. By applying the volume average method on Eq. (2), the volume-averaged strain on the I^{th} phase is obtained as

$$\bar{\boldsymbol{\varepsilon}}^{I} = \boldsymbol{\varepsilon}^{r}_{macro} - \sum_{J=0}^{N} \frac{1}{\Omega_I}\int_{\Omega_I}\int_{\Omega_J} \boldsymbol{\xi}(\vec{\boldsymbol{r}} - \vec{\boldsymbol{r}_J})d\Omega_J d\Omega_I : \delta\boldsymbol{C}^{J}_{fluc}: \boldsymbol{\varepsilon}^{J}_{micro} \tag{3}$$

where N is the number of inclusion phases. The interaction tensor $\boldsymbol{T}^{IJ}$ that characterizes the interaction properties between the I^{th} phase and the J^{th} phase of the composite is proposed by Fehri *et al.* (Fassi-Fehri 1985) as follows

$$\boldsymbol{T}^{IJ} = \frac{1}{\Omega_I}\int_{\Omega_I}\int_{\Omega_J} \boldsymbol{\xi}\left(\vec{\boldsymbol{r}} - \vec{\boldsymbol{r}_J}\right)d\Omega_J d\Omega_I, \tag{4}$$

The local strain concentration tensor $\boldsymbol{b}^{I}(\vec{\boldsymbol{r}})$ that connects the macroscopic strain $\boldsymbol{\varepsilon}^{r}_{macro}$ to the average strain field within the I^{th} inclusion is expressed as

where the bracket <·> is the volume averaged quantity. Combining the Eq. (3)-(6), the local strain concentration tensor $\boldsymbol{b}^I(\vec{\boldsymbol{r}})$ is obtained with iterations through Eq. (7)

$$\boldsymbol{b}_{i+1}^I(\vec{\boldsymbol{r}}) = [\boldsymbol{I} + \boldsymbol{T}^{II}\colon(\boldsymbol{C}^I - \boldsymbol{C}^{\boldsymbol{0}})]^{-1}\colon\left[I - \sum_{\substack{J=0,\\ J\neq I}}^{N} \boldsymbol{T}^{IJ}\colon(\boldsymbol{C}^J - \boldsymbol{C}^0)\colon\boldsymbol{b}_i^I(\vec{\boldsymbol{r}})\right] \tag{7}$$

Herein, $\boldsymbol{b}_i^I(\vec{\boldsymbol{r}})$ is the local strain concentration tensor at i-th iteration and $\boldsymbol{C}^0$ is the stiffness of the surrounding matrix.

In the particular case that the composite material consists of the matrix phase and one inclusion phase, the interaction tensor $\boldsymbol{T}^{II}$ and the effective stiffness tensor $\boldsymbol{C}_{macro}^{eff}$ is expressed

$$\boldsymbol{T}^{II} = \boldsymbol{S}\colon(\boldsymbol{C}^0)^{-1} \tag{8}$$

$$\boldsymbol{C}_{macro}^{eff} = \sum_{I=0}^{N} v_I\,\boldsymbol{C}^I\colon\boldsymbol{B}^I = v_0\boldsymbol{C}^0\colon\boldsymbol{B}^0 + \sum_{I=1}^{N} v_I\,\boldsymbol{C}^I\colon\boldsymbol{B}^I \tag{9}$$

where $\boldsymbol{S}$ is the Eshelby tensor, and v_0 and v_I are the volume fractions of the matrix phase and inclusion phase, respectively. For the case that there is an interface layer between the inclusion phase and matrix phase, the modified Eshelby tensor $\boldsymbol{S}^M$ is used instead of the Eshelby tensor $\boldsymbol{S}$ to reflect the imperfectly bonded interfacial effect of the composites. The modified Eshelby tensor is given as

$$\boldsymbol{S}^M = \boldsymbol{S} + (\boldsymbol{I} - \boldsymbol{S})\colon\boldsymbol{H}\colon\boldsymbol{C}^0\colon(\boldsymbol{I} - \boldsymbol{S}) \tag{10}$$

For spherically shaped inclusions, the fourth-order tensor $\boldsymbol{H}$ that contains interfacial information with interfacial sliding and normal debonding parameters, $\boldsymbol{P}$ and $\boldsymbol{Q}$ are given as

$$\begin{gathered}\boldsymbol{H} = \alpha\boldsymbol{P} + (\beta - \alpha)\boldsymbol{Q} \\ P_{ijkl} = \frac{1}{a}I_{ijkl}, \quad Q_{ijkl} = \frac{1}{5a}(2I_{ijkl} + \delta_{ij}\delta_{kl})\end{gathered} \tag{11}$$

Herein, α and β are the shear and normal compliance parameters, respectively for the interphase layer material properties. α and β are expressed in terms of the interphase thickness t and the interphase layer's shear moduli μ_i and bulk moduli K_i as

$$\alpha = \frac{t}{\mu_i}, \qquad \beta = \frac{t}{(K_i + \frac{4\mu_i}{3})} \tag{12}$$

Assuming that the matrix phase material shows the viscoelastic material characteristics, the time-dependent constitutive matrix of the matrix phase $\boldsymbol{C}_{ijkl}^0$ is obtained as

$$\boldsymbol{C}_{ijkl}^0 = \left[k_m(t) - \frac{2}{3}\mu_m(t)\right]\delta_{ij}\delta_{kl} + \mu_m(t)(\delta_{ik}\delta_{jl} + \delta_{il}\delta_{jk}) \tag{13}$$

Herein, k_m and μ_m are the bulk and shear moduli for matrix phase while δ is an Kronecker delta with i, j, k, l basis. Finally, by combining Eqs. (7)-(10), the effective stiffness of the particulate composite is obtained as

$$\boldsymbol{C}^{MT\,eff} = \left[\left(1-v_p\right)\boldsymbol{C}^0 + v_p\boldsymbol{C}^p{:}\,\boldsymbol{b}^p\right]{:}\left[\left(1-v_p\right)\boldsymbol{I} + v_p(\boldsymbol{I}+\boldsymbol{H}^p{:}\,\boldsymbol{C}^p){:}\,\boldsymbol{b}^p\right]^{-1} \tag{14}$$

where the superscript p implies particle phase. Herein, $\boldsymbol{C}^{MT\,eff}$ is an effective stiffness of the particulate composite obtained by Mori-Tanaka homogenization approach. The stress prediction of the particulate composite is obtained by adopting the viscoelastic constitutive relation as

$$\boldsymbol{\sigma}_{ij}(t) = \int_0^t \boldsymbol{C}_{ijkl}^{MT\,eff}(t-s){:}\frac{\partial \boldsymbol{\varepsilon}_{kl}^{macro}(s)}{\partial s}ds \tag{15}$$

The constitutive equation in Eq. (15) is converted to the finite difference form to obtain stress value numerically. The constitutive equation shows a stress relaxation effect by relaxing the effective stress and response delay effect using the Boltzmann integral form. In this paper, we proposed Eq. (15) to propose the new homogenization methodology that predicts the effective stress of the viscoelastic particulate composites. The nonlinear material behavior of composites appears as the effective constituent matrix changes as the matrix stiffness changes.

3. Verification of the micromechanics model

This section presents verification of the present viscoelastic micromechanics model with the finite element-based DNS model. The DNS model is conducted with a commercial software ABAQUS and compared with the proposed micromechanics model. The effects of composite constituents' properties on the viscoelastic behavior will be presented in Section 4.

3.1 DNS finite element models

Fig. 2 shows the geometries and FE meshes for the eight DNS models. The generated FE models are divided into models with an interphase layer and models without an interphase layer having different volume fractions 5%, 10%, 15%, and 20%. The finite element models are developed with the solid element (C3D8 in ABAQUS), and a total of 125,000 voxel elements (50×50×50) are used. Although the mesh sensitivity analysis is not performed, the further refined 50×50×50 mesh quality was checked that improves consistent results compared to a coarse mesh 20×20×20. The physical dimension of the model is 1 mm×1 mm×1 mm. It is well known that the stress prediction according to the Mori-Tanaka homogenization method is equivalent if the volume fraction and the shape of inclusion is equal whether there are single inclusions or multiple inclusions (Liu and Huang 2014). Therefore, we have used DNS model with single inclusion in this research to validate the proposed homogenization model.

3.2 Boundary conditions and material properties

The periodic boundary condition utilized to estimate the effective mechanical properties (Taheri-Behrooz and Pourahmadi 2019, Pourahmadi and Taheri-Behrooz 2020) is applied to the DNS models. Fig. 3 shows the schematics of the given boundary conditions for the finite element model. Cyclic triaxial strain loading conditions with a frequency $f = 2$ Hz are applied for the x, y, z-directions as in Eq. (16)

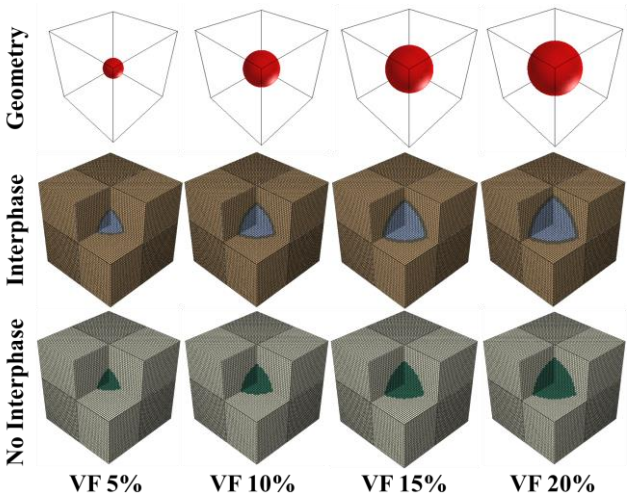

Fig. 2 Finite element modeling for DNS

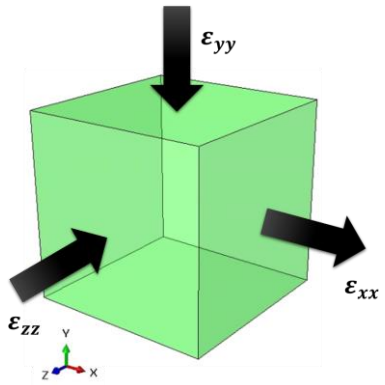

Fig. 3 Schematics of the boundary conditions for the finite element model

$$\boldsymbol{\varepsilon}_{ij}^{macro} = \begin{bmatrix} 0.1 & 0 & 0 \\ 0 & -0.05 & 0 \\ 0 & 0 & -0.05 \end{bmatrix} sin(2\pi f t) \tag{16}$$

The material parameters for the DNS model are summarized in Table 1. The linear elastic materials' properties are used for fiber phase and interphase layer (Lim *et al.* 2020) while the viscoelastic materials' parameters are used for matrix phase. Here, $\mathrm{E_p}$ and $\mathrm{E_i}$ are Young's moduli of the particle and interphase layer, respectively. $E_{\mathrm{m}}^{\mathrm{t=0}}$ is the matrix's Young's modulus at time t=0. Poisson ratio of the particle (ν_{p}) and the interphase layer (ν_{i}) is assumed to be 0.4. Assuming the interphase layer's thickness is a 0.15 mm, corresponding α and β value is 0.042 and 0.07 according to the Eq. (12). The thickness of the interphase layer is equal to 0.15 times of the radius and therefore differs according to the volume fraction. The thickness of the interfacial layer is 0.0342 mm, 0.0431 mm, 0.0494 mm, and 0.0544 mm depending on the 5%, 10%, 15%, and 20% volume fractions. The viscoelastic material parameters of the matrix for the simulation is determined to be relaxed as half at time t=1 and Young's modulus at time t=0 is determined to 10 as a reference value for easily comparing the stiffness of the constituents.

Table 1 Independent material's parameters for DNS

	E_p [MPa]	ν_p	E_i [MPa]	ν_i	$E_m^{t=0}$ [MPa]
Model without the Interphase layer	5	0.4	-	-	10
Model with the Interphase layer	5	0.4	10	0.4	10

Table 2 Generalized Maxwell parameters for the viscoelastic micromechanics model

Matix							
$E_m^{t=0}$ (MPa)	ν_m	μ_1 (MPa)	μ_2 (MPa)	μ_3 (MPa)	τ_1 (s)	τ_2 (s)	τ_3 (s)
10	0.4	1.4285	1.0714	1.0714	0.2	0.15	0.15

3.3 Viscoelastic micromechanics model

Like the DNS models, a total of eight viscoelastic micromechanics models were constructed with and without interphase layer and four different volume fractions (5%, 10%, 15%, and 20%). The viscoelastic material parameters for the matrix phase are shown in Table 2. Here, μ and τ are the viscoelastic material parameters of the Maxwell elements (Gillani 2018). The Poisson ratio of the matrix (ν_m) is assumed to be 0.4.

3.4 Verifications

The proposed viscoelastic micromechanics models are verified with the DNS model in terms of von-Mises stresses and equivalent strain cyclic responses. The stress-strain data of the DNS are obtained for 50 points with a time interval of 0.02 sec. The stress prediction error (*Err*) of the micromechanics method is obtained by summing the absolute errors at 50 points and dividing it by the number of total points as follows

$$Err = \sum_{k=1}^{50} \frac{|\sigma_v^H(t_k) - \sigma_v^{DNS}(t_k)|}{\sigma_v^{DNS}(t_k) \times 50} \tag{17}$$

where *t* is the analysis time and *k* is the time index for the proposed micromechanics model and DNS analysis points. $\sigma_v^H(t_k)$ and $\sigma_v^{DNS}(t_k)$ are the volume-averaged von-Mises stress obtained by the proposed micromechanics model and DNS, respectively. Fig. 4 shows the stress prediction error of the proposed micromechanics model according to the volume fractions. The stress prediction error increases as the volume fraction of the composite increases, and the model with the interphase layer shows better prediction accuracy. It is well known that the accuracy of the Mori-Tanaka method decreases rapidly as the volume fraction of the composites increases (Christensen *et al.* 1992). The proposed micromechanics model also shows the same tendency in the perspective of prediction accuracy. The stress prediction error of the proposed micromechanics model is below 2.5% when the interphase layer is considered. In addition, if the stiffness of the particle phase is similar to the stiffness of the matrix phase, the accuracy of the micromechanics model becomes more accurate.

Fig. 5 shows contours of the maximum principal strain of DNS and the stress-strain curve obtained with the proposed micromechanics model and DNS for the model with and without

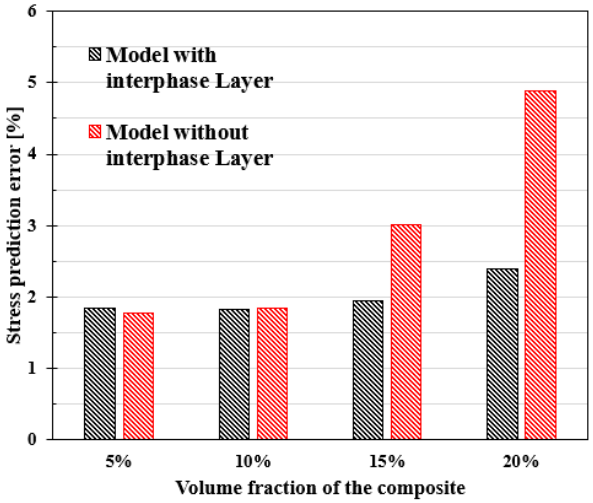

Fig. 4 Stress prediction error according to the volume fraction

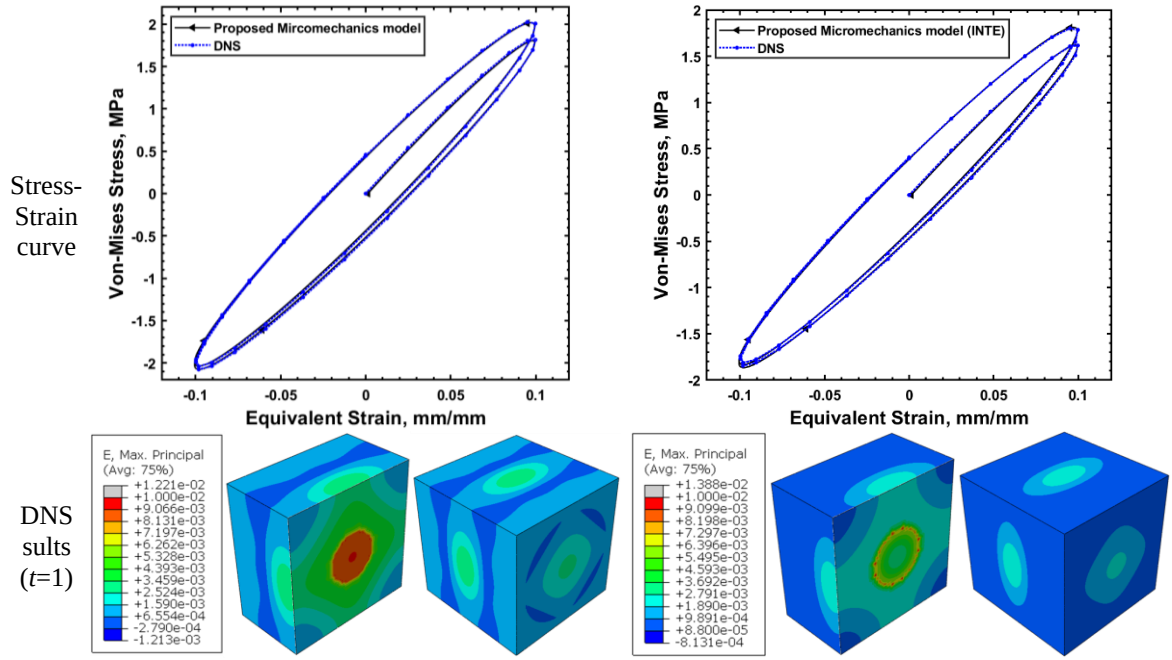

(a) Model without interphase layer; V_f : 5%, $E_m^{t=0}$: 10MPa, E_p: 5MPa

(b) Model with an interphase layer; V_f : 5%, $E_m^{t=0}$: 10MPa, E_p: 5MPa, E_i: 10MPa

Fig. 5 Stress-strain curve and DNS results, V_p: 5%

interphase layer (V_p: 5%). Since it is to show validation of the proposed homogenization method's prediction, the stiffness of the matrix (10 MPa) is larger than stiffness of the fiber (5MPa). The curves show that the stress prediction with the proposed micromechanics model is almost identical to DNS results. The prediction error for the model without an interphase layer (V_p: 5%) and the

model with an interphase layer (V_p: 5%) are 1.77% and 1.84% respectively. The author's previous research also shows the numerical validation of the proposed homogenization method for tangent delta properties and the stress relaxation effect according to the time (You *et al.* 2021).

4. Effects of constituents' properties, volume fraction and interfacial imperfection on the viscoelastic behavior

This section presents the effects of the constituent's properties, volume fraction, and interfacial imperfection on the viscoelastic behavior of the composites. One of the critical parameters for dynamic mechanical properties, the Tangent delta (tan δ), is estimated by the phase difference between the stress and strain. Moreover, the relaxation effect of composites is examined. The tan δ and relaxation according to the constituents' properties, volume fraction, and interfacial layer and their effect, are investigated.

4.1 Effect of constituents' properties on relaxation effect

The effect of the constituents' properties on the composites' relaxation is examined. Fig. 6 shows the relaxation of the composite according to the stiffness ratio ($E_p/E_m^{t=0}$). The loading condition is applied as follows

$$\boldsymbol{\varepsilon}_{ij}^{macro} = \begin{bmatrix} 0.1 & 0 & 0 \\ 0 & -0.05 & 0 \\ 0 & 0 & -0.05 \end{bmatrix} \times 50 \times t\,, \quad when\ (t < 0.02s) \tag{18}$$

The volume fraction is fixed to 10%, and the interphase layer is not considered. The results can be used by calibrating it to the viscoelastic material parameters and applying it to the commercial FE solver. It is worth noting that the composites' relaxation behavior is largely affected by the stiffness ratio. The inclusion stiffness contributes to the reinforcing effect. Therefore, only the stress magnitudes increase whereas the relaxation behavior does not change.

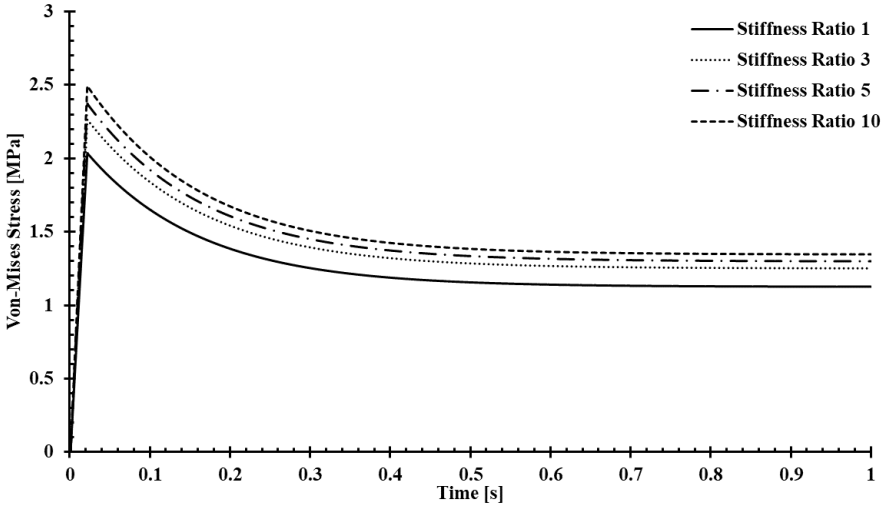

Fig. 6 Relaxation behavior of composite according to the constituents' properties

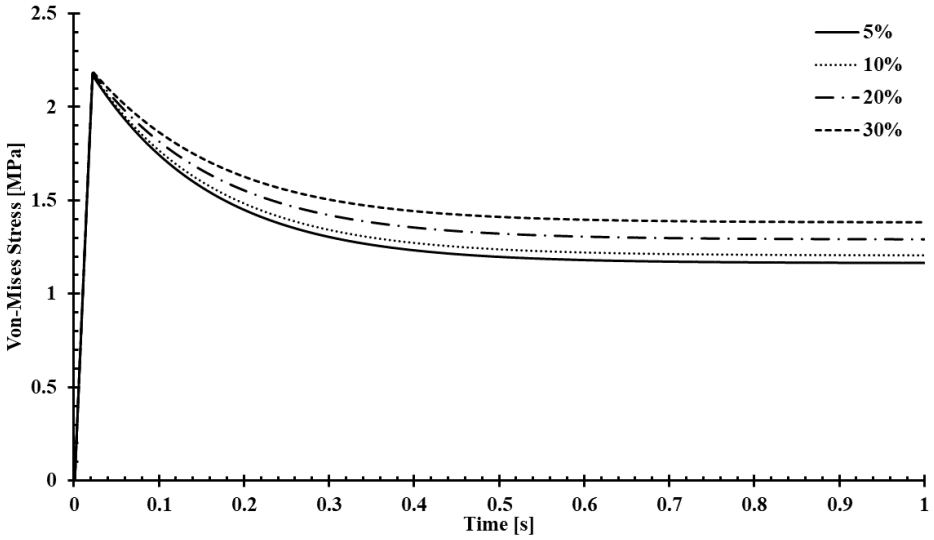

Fig. 7 Relaxation behavior of composite according to the volume fraction

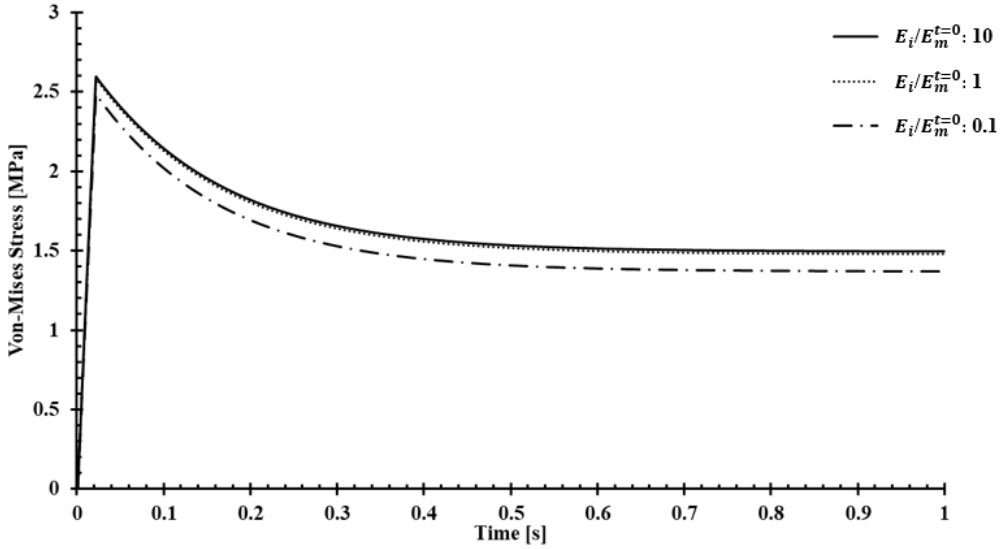

Fig. 8 Relaxation behavior of composite according to the interphase layer

4.2 Effect of volume fraction on relaxation effect

The effect of the volume fraction on the composites' relaxation is investigated. Fig. 7 shows the relaxation of the composite according to the volume fractions of the composites. The stiffness ratio ($E_p/E_m^{t=0}$) is fixed to 2 and the loading condition in Eq. (18) is applied. The result shows that the stress relaxation of the composite slows down as the volume fraction increases. It is because only the matrix shows the viscoelastic behavior. Also, there is a difference in the stresses before relaxation depending on the volume fraction, but is not distinguishable on the figure due to the small stress ratio.

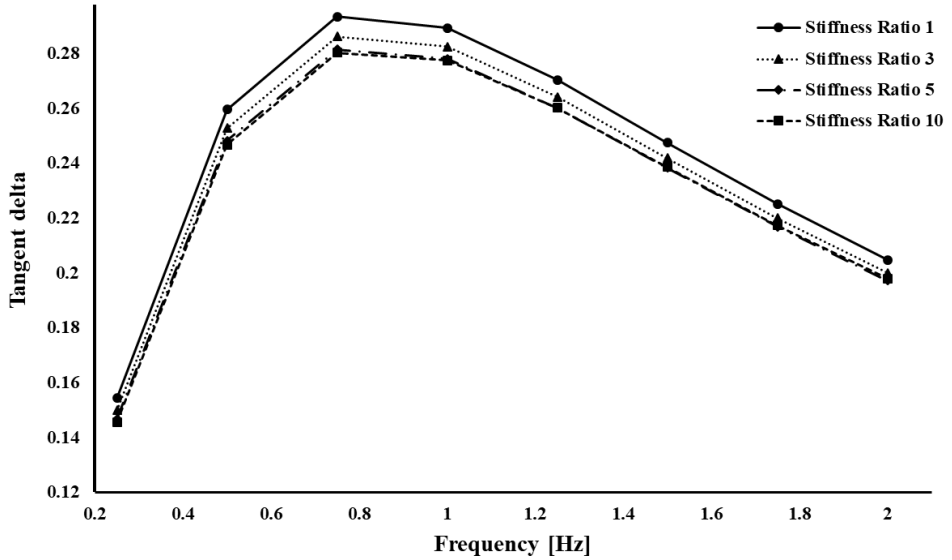

Fig. 9 tan (δ) according to the stiffness ratio

4.3 Effect of interfacial imperfection on relaxation effect

Fig. 8 shows the relaxation behavior of the composites according to the interfacial imperfection. The volume fraction of the composites is fixed to 20% while the stiffness ratio ($E_p/E_m^{t=0}$) is fixed to 5. The same loading condition is applied. Since the difference of relaxation behavior according to the interfacial imperfection was small, the interphase layer's material property ratio ($E_i/E_m^{t=0}$) is varied from 0.1 to 10 so that the difference between models can be observed clearly.

4.4 Effect of constituents' properties on tangent delta

The effect of the constituents' properties on tan δ is examined, as shown in Fig. 9. To observe the effect of constituents' properties, the stiffness ratio ($E_p/E_m^{t=0}$) is varied while the volume fraction is fixed to 10%, and no interphase layer is assumed. The result shows a clear tendency that the tangent delta of the composite becomes higher as the stiffness ratio decreases.

4.5 Effect of volume fraction on tangent delta

The effect of the volume fraction on tan (δ) is shown in Fig. 10. The volume fraction is varied from 5% to 20%, while the stiffness ratio is fixed to 5, and no interphase layer is assumed. The result shows that the tangent delta decrease when the volume fraction increases. This result makes sense with a common phenomenon that a composite loses the viscoelastic characteristics as the volume fraction increases.

4.6 Effect of interfacial imperfection on tangent delta

To observe the effect of the interphase layer effect on tan (δ), the stiffness ratio is fixed to 10, and the volume fraction is fixed to 10%, while the interphase layer's material property ratio ($E_i/E_m^{t=0}$)

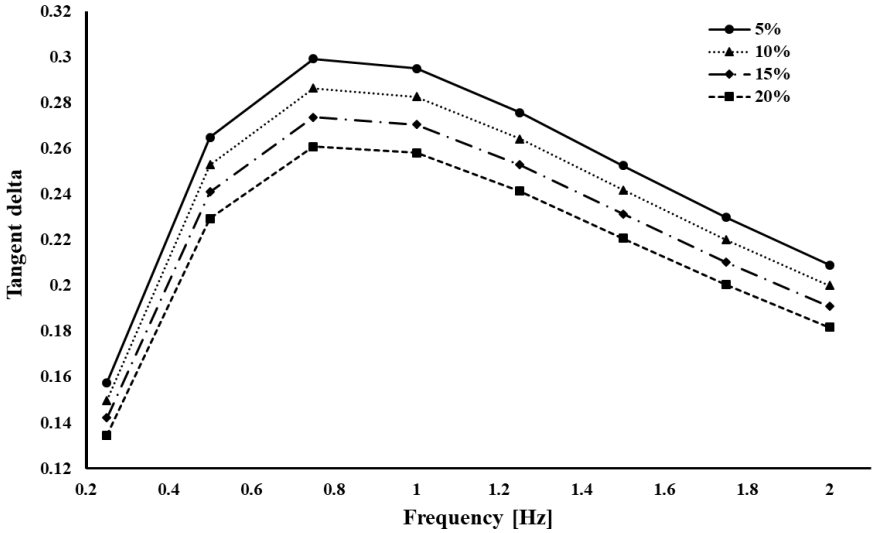

Fig. 10 tan (δ) according to the volume fraction

Table 3 tan (δ) according to the interphase layer properties

$E_i/E_m^{t=0}$ / Frequency (Hz)	1	2	3	4	5
0.5	0.2611	0.2604	0.2602	0.2600	0.2599
1	0.2909	0.2902	0.2899	0.2898	0.2897
2	0.2059	0.2054	0.2053	0.2051	0.2050

is varied from 1 to 5. Table 3 shows the tan (δ) value according to the $E_i/E_m^{t=0}$. It is noticed that the effect of the interphase layer is small, compared to the effect of volume fraction and stiffness ratio of matrix and particle. At each frequency, the tan (δ) value slightly decreases as the ratio ($E_i/E_m^{t=0}$) increases.

4.7 Results and discussions for viscoelastic behavior

The effects of constituents' properties, volume fraction, and interfacial imperfection on dynamic mechanical behavior and the relaxation effect of the viscoelastic composites are examined with the proposed micromechanics model. As shown in Fig. 6 and 7, although the stress magnitude seems to be proportional to the stress stiffness ratio, the rate of stress relaxation are identical. It is because the viscoelastic behavior is mainly dependent on the volume fraction of the resin. Fig. 8 shows the interphase stiffness can influence both the rate of stress relaxation and the stress magnitude. The interphase material generally has higher density than polymer resin and the inclusion could increase the shear modulus of the interphase layer (Park and Yun 2018). Considering this, the interphase layer provides an effect of decreasing resin's volume fraction. Comparing the Figs. 9 and 10, and Table 3, the volume fraction is a dominant factor that affects the dynamic mechanical property of the viscoelastic composites. Fig. 9 shows that the tangent delta increases as the particle becomes stiffer. These results make sense considering that the tangent delta has a physical meaning that is a ratio of

viscosity and elasticity. As the particle becomes stiffer, the elasticity of the system increases and therefore the tangent delta decreases. Table 3 shows that the tangent delta value decreases as the interphase layer becomes stiffer. As the interphase layer becomes stiffer, the elasticity of the system slightly increases and therefore the tangent delta decreases. However, the effect of the interphase layer was not significant. Although the proposed micromechanics model can consider the constituent's mechanical property, volume fraction and interfacial imperfection of viscoelastic composites, it still has limitations on the physical explanation of the results since it is a phenomenological model that does not explain a molecular movement of viscoelastic material. The free volume theory proposed by Carl *et al.* is referred to provide insight and support to the physical explanation of this result (Popelar and Liechti 2003). According to the free volume theory, the viscoelastic material behavior can be explained from the perspective of molecular chain mobility. In detail, the mechanical behavior of viscoelastic materials composed of a large number of entangled polymer chains can be influenced by the "free volume", the remaining volume between polymer chains that determines the mobility of the molecular chains (Popelar and Liechti 2003). Fig. 10 shows the peak of the tangent delta value becomes lower as the volume fraction of the composites increases. Although this result is obtained by proposed micromechanics model which is a phenomenological model, it can also be explained in respect to molecular chain mobility. From the point of view of the free volume theory, it can be explained that as the volume fraction increases, the free volume inside the material system decreases, which makes the lower molecular chain mobility and loosen the viscoelastic material characteristics.

5. Conclusions

The mean-field-based micromechanics model is presented with the basic micromechanics theory. The present mean-field-based micromechanics model utilizes the Mori-Tanaka theory and viscoelastic constitutive relation. After showing the theoretical implementation of the micromechanics model, DNS is conducted to validate the micromechanics model. Authors generated the finite element model with different volume fractions, material properties, and interphase layers for DNS, which is used to investigate the stress prediction error of the micromechanics model. The results show that the higher the volume fraction, the higher the stress prediction error. Lastly, the effects of the constituent's properties, volume fraction, and interfacial imperfection on the dynamic mechanical behavior of the composites are examined. The results show that the effect of volume fraction of the composite on the dynamic mechanical property is dominant compared to the constituent's properties and interphase layer effect examined in this paper.

- The micromechanics model for the viscoelastic composites is presented with Eshelby's inclusion theory and the Mori-Tanaka homogenization method.
- The numerical validation of the proposed micromechanics model is conducted by DNS with the commercial software ABAQUS.
- The stress prediction accuracy according to the volume fraction of the viscoelastic composites is estimated.
- The effects of volume fraction, constituents properties, and interfacial imperfection on viscoelastic material is investigated.
- The effects of volume fraction of the viscoelastic composites on relaxation behavior and dynamic mechanical property is dominant according to the proposed micromechanics model.

Acknowledgments

This work was supported by the Institute of Engineering Research of Seoul National University, Hankook Tire and Technology Co. Ltd and U.S. Air Force Office of Scientific Research under award number FA2386-20-1-4067. Authors are grateful for the supports.

References

Khajehsaeid, H., Arghavani, J., Naghdabadi, R. and Sohrabpour, S. (2014), "A visco-hyperelastic constitutive model for rubber-like materials: A rate-dependent relaxation time scheme", *Int. J. Eng. Sci*., **79**, 44-58. https://doi.org/10.1016/j.ijengsci.2014.03.001.

Oleiwi, J.K., Hamza, M.S. and Nassir, N.A. (2011), "A study of the effect of carbon black powder on the physical properties of SBR/NR blends used in passenger tire treads", *Eng. Tech. J*., **29**(5), 856-870.

Li, X., Li, Z. and Xia, Y. (2015), "Test and calculation of the carbon black reinforcement effect on the hyper-elastic properties of tire rubbers", *Rubber Chem. Tech*., **88**(1), 98-116. https://doi.org/10.5254/rct.14.86932.

Khadimallah, M.A., Safeer, M., Taj, M., Ayed, H., Hussain, M., Bouzgarrou, S.M. and Tounsi, A. (2020), "The effects of the surrounding viscoelastic media on the buckling behavior of single microfilament within the cell: A mechanical model", *Adv. Concrete Constr*., **10**(2), 141-149. http://doi.org/10.12989/acc.2020.10.2.141.

Patnaik, S.S., Swain, A. and Roy, T. (2020), "Creep compliance and micromechanics of multi-walled carbon nanotubes based hybrid composites", **2**(2), 141. http://doi.org/10.12989/cme.2020.2.2.141.

Park, C., Kim, G., Jung, J., Krishnakumar, B., Rana, S. and Yun, G.J. (2020), "Enhanced self-healing performance of graphene oxide/vitrimer nanocomposites: A molecular dynamics simulations study", *Polym*., **206**, 122862. https://doi.org/10.1016/j.polymer.2020.122862.

Shao, H.Q., Wei, H. and He, J.H. (2018), "Dynamic properties and tire performances of composites filled with carbon nanotubes", *Rubber Chem. Tech*., **91**(3), 609-620. https://doi.org/10.5254/rct.18.82599.

Zhao, W., Liu, L., Leng, J. and Liu, Y. (2019), "Thermo-mechanical behavior prediction of particulate reinforced shape memory polymer composite", *Compos. Part B Eng*., **179**, 107455. https://doi.org/10.1016/j.compositesb.2019.107455.

Hashin, Z. (1965), "Viscoelastic behavior of heterogeneous media", *J. Appl. Mech*., **32**(3), 630-636. https://doi.org/10.1115/1.3627270.

Christensen, R.M. (1969), "Viscoelastic properties of heterogeneous media", *J. Mech. Phys. Solid*., **17**(1), 23-41. https://doi.org/10.1016/0022-5096(69)90011-8.

Hashin, Z.V.I. (1970), "Complex moduli of viscoelastic composites-I. General theory and application to particulate composites", *Int. J. Solid. Struct*., **6**(5), 539-552. https://doi.org/10.1016/0020-7683(70)90029-6.

Laws, N. and McLaughlin, R. (1978), "Self-consistent estimates for the viscoelastic creep compliances of composite materials", *Proceedings of the Royal Society of London, Mathematical and Physical Sciences*, **359**(1697), 251-273. https://doi.org/10.1098/rspa.1978.0041.

Brinson, L.C. and Lin, W.S. (1998), "Comparison of micromechanics methods for effective properties of multiphase viscoelastic composites", *Compos. Struct*., **41**(3-4), 353-367. https://doi.org/10.1016/S0263-8223(98)00019-1.

Lahellec, N. and Suquet, P. (2007), "Effective behavior of linear viscoelastic composites: a time-integration approach", *Int. J. Solid. Struct*., **44**(2), 507-529. https://doi.org/10.1016/j.ijsolstr.2006.04.038.

Chen, Y., Yang, P., Zhou, Y., Guo, Z., Dong, L. and Busso, E.P. (2020), "A micromechanics-based constitutive model for linear viscoelastic particle-reinforced composites", *Mech. Mater*., **140**, 103228. https://doi.org/10.1016/j.compstruct.2021.113679.

Dederichs, P.H. and Zeller, R. (1973), "Variational treatment of the elastic constants of disordered materials", *Zeitschrift für Physik A Hadrons and nuclei*, **259**(2), 103-116. https://doi.org/10.1016/0022-5096(88)90001-4.

Fassi-Fehri, O. (1985), "Le problème de la paire d'inclusions plastiques et hétérogènes dans une matrice anisotrope: Application à l'étude du comportement des matériaux composites et de la plasticité", Doctoral Dissertation of Philosohpy, Université Paul Verlaine-Metz.

Liu, L. and Huang, Z. (2014), "A note on Mori-Tanaka's method", *Acta Mechanica Solida Sinica*, **27**(3), 234-244. https://doi.org/10.1016/S0894-9166(14)60033-1.

Taheri-Behrooz, F. and Pourahmadi, E. (2019), "A 3D RVE model with periodic boundary conditions to estimate mechanical properties of composites", *Struct. Eng. Mech.*, **72**(6), 713-722. https://doi.org/10.12989/sem.2019.72.6.713.

Pourahmadi, E. and Taheri-Behrooz, F. (2020), "The influence of fiber bundle width on the mechanical properties of filament-wound cylindrical structures", *Int. J. Mech. Sci.*, **178**, 105617. https://doi.org/10.1016/j.ijmecsci.2020.105617.

Lim, H.J., Choi, H., Zhu, F.Y., Kerekes, T.W. and Yun, G.J. (2020), "Multiscale damage plasticity modeling and inverse characterization for particulate composites", *Mech. Mater.*, **149**, 103564. https://doi.org/10.1016/j.mechmat.2020.103564.

Gillani, A. (2018), "Development of material model subroutimes for linear and non linear response of elastomers", University of Western Ontario.

Christensen, R., Schantz, H. and Shapiro, J. (1992), "On the range of validity of the Mori-Tanaka method", *J. Mech. Phys. Solid.*, **40**(1), 69-73. https://doi.org/10.1016/0022-5096(92)90240-3.

You, H., Lim, H., Choi, H. and Yun, G. (2021), "Prediction of viscoelastic behavior of particulate composites by a time-Domain homogenization approach", *AIAA Scitech 2021 Forum*.

Park, C. and Yun, G.J. (2018), "Characterization of interfacial properties of graphene-reinforced polymer nanocomposites by molecular dynamics-Shear deformation model", *J. Appl. Mech.*, **85**(9), 091007. https://doi.org/10.1115/1.4040480.

Popelar, C.F. and Liechti, K.M. (2003), "A distortion-modified free volume theory for nonlinear viscoelastic behavior", *Mech. Time-Dependent Mater.*, **7**(2), 89-141. https://doi.org/10.1023/a:1025625430093.

CC